A detailed study on optimizing DMLS process parameters to enhance AlSi10Mg metal component properties

Pragnya Kunisetti[1*] and Balla Srinivasa Prasad[1]

*Correspondence:
pragnyak1332@gmail.com

[1] Department of Mechanical Engineering, GITAM School of Technology, GITAM, Visakhapatnam, India

Abstract

This study investigates the effects of laser power, scan speed, and hatch distance on the features of aluminium specimens produced using direct metal laser sintering (DMLS). By systematically varying these parameters, we identified optimal combinations for producing high-quality metal components. Our findings were validated through reproducible printing processes. Analysis of variance (ANOVA) and grey relational analysis (GRA) were employed to optimize the production parameters further. We found a significant trade-off between laser power, tensile strength, and fatigue resistance, with laser power having the most substantial impact on mechanical properties, microstructure, and surface roughness. Statistical analysis confirmed that higher laser power improves mechanical characteristics but may increase surface roughness. These insights are crucial for enhancing the efficiency and quality of DMLS-produced metal components.

Keywords: Direct metal laser sintering, Analysis of variance, Taguchi techniques, Aluminum composites, Grey relational analysis, Scanning electron microscope

Introduction

Direct metal laser sintering (DMLS) melts and fuses metal powder particles to build items layer by layer in additive manufacturing [1]. It is an advanced additive manufacturing process ideal for producing high-precision, complex metal parts from AlSi10Mg, an aluminum alloy with silicon and magnesium. This process is particularly beneficial for creating intricate geometries, rapid prototyping, and low-volume production, eliminating the need for expensive tooling and molds. From design preparation to post-processing and inspection, the procedure is meticulous [2]. To avoid distortion, optimise layer-by-layer production, and strategically place support structures [3–6]. Material selection is essential for mechanical and functional needs. Proper powder bed preparation guarantees quality and uniformity [7]. This strong laser melts metal powder particles using a predefined scanning approach. Laser beam diameter and scanning speed must be controlled for accurate melting and solidification. Final component microstructure and mechanical characteristics are affected by controlled cooling [8]. Considerations for DMLS include the use of support structures, post-processing steps like

stress relief and surface finishing, proper build orientation, and layer thickness to ensure optimal mechanical properties and dimensional accuracy. Complex geometries need support structures for heat dissipation and powder dispersion as design optimisation reduces support structures. The study analyses AlSi10Mg powder DMLS mechanical properties and surface features using ANOVA and signal-to-noise ratio analysis. The research examines DMLS-produced aluminium components before and after corrosion and uses FESEM for material analysis to bridge the knowledge gap.

Materials and Experimental Procedure

Materials

The EOS M 290 uses DMLS to sinter AlSi10Mg and AlSi powders. AlSi10Mg offers properties such as lightweight, high strength-to-weight ratio, good thermal conductivity, corrosion resistance, and excellent ductility and toughness. DMLS meets the need for precision, customization, material efficiency, and tool-less manufacturing, reducing costs and lead times while enabling complex designs without added expense. Aluminium alloys have become a cornerstone in modern engineering, offering a blend of cost-effectiveness and high performance that meets the demanding requirements of various applications. Among these, the AlSi matrix stands out, particularly the AlSi10Mg alloy, which has gained significant traction in the industry for its exceptional mechanical properties and versatility. The manufacturing of AlSi10Mg components has been revolutionized with the advent of direct metal laser sintering (DMLS) technology. DMLS allows for the creation of complex geometrical shapes and thin-walled structures with high precision and consistency. This additive manufacturing technique has further enhanced the appeal of AlSi10Mg, enabling the production of intricate parts that would be challenging or even impossible to manufacture using traditional methods. By utilizing DMLS for AlSi10Mg, manufacturers can achieve high-quality, complex metal parts suited for aerospace, automotive, and industrial applications, meeting stringent performance demands.

Table 1 shows the recommended AlSi10Mg chemical composition [5].
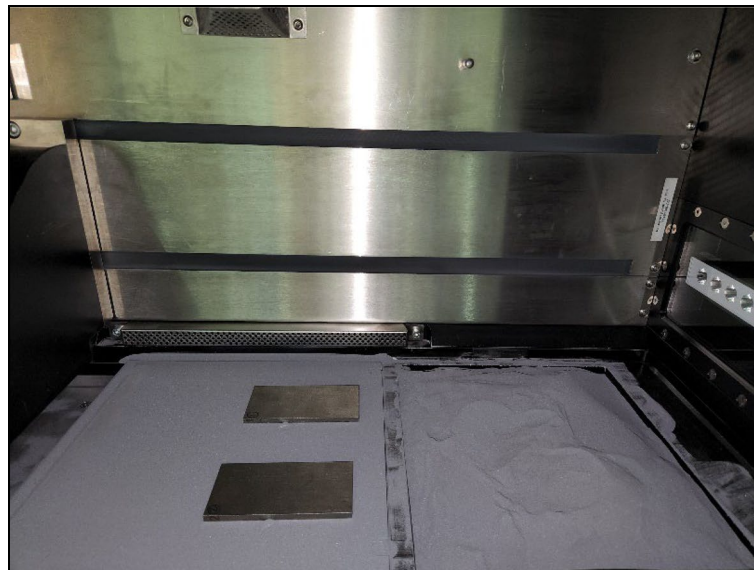
Experimental Procedure

The EOS M 290 machine selectively sinters metal powders in thin layers 20–40 microns thick using a 400-Watt Yb fibre laser and F–Theta focusing lens to match the part's cross-sectional shape from a digital CAD model. Its construction envelope is $325 \times 250 \times 250$ mm. Experimental procedure is schematically represented in Fig. 1a. The DMLS machine uses a specific way to move the laser beam over a bed of powder, following the shape of a computer-designed model. This melts the powder in the right spots accurately. The machine's settings, like the size of the beam, how fast it moves, and its power, are chosen based on what the part needs. When the laser heats the powder, it melts it, and as it moves, the melted material hardens, making a layer. This keeps happening until the whole part is made. The laser's power and speed need to be controlled together to get the right amount of heat. As each layer cools, it affects the final part's quality as shown in Fig. 1b. Support structures are important in DMLS, especially for tricky parts. They hold up parts as they're made, help with cooling, and make sure the powder spreads evenly. They also make it easier to clean up excess powder afterward. An entire process for which DMLS EOS M290 is used in carrying out experiments to figure

Table 1 AlSi10Mg particles chemical composition

Element	Al	Si	Mg	Fe	Cu	Mn	Zn	Ti	Ni	Pb
Concentration weight %	Balance	9.0–11.0	0.2–0.45	Max. 0.55	Max. 0.05	Max. 0.45	Max. 0.1	Max. 0.15	Max. 0.05	Max. 0.05
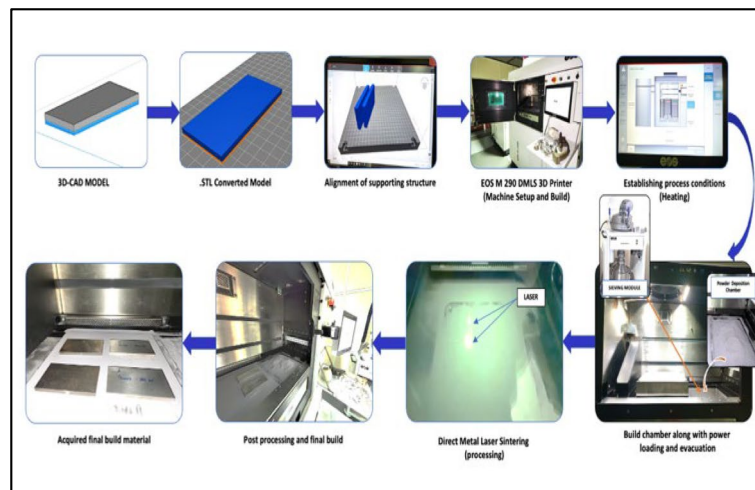
(a): Experimental procedure

(b): Prepared specimen

Fig. 1 **a** Experimental procedure. **b** Prepared specimen

out how different factors affect the quality of parts made with DMLS using AlSi10Mg powder of 3 to 50 microns. The powder particles are predominantly spherical, promoting excellent flowability and high packing density, essential for consistent layer deposition in direct metal laser sintering (DMLS). The fine particle size distribution ensures a smooth surface finish and detailed feature resolution in the printed parts. Additionally, the powder has a thin oxide layer that protects against further oxidation and maintains high purity levels, ensuring consistent thermal and mechanical properties. Its high thermal conductivity and specific heat capacity aid in efficient heat dissipation during the laser melting process, minimizing thermal gradients and residual stresses in the final product. They looked at things like hardness, strength, and how rough the surface was

[9]. Systematic experimentation optimises sintered aluminium samples' quality, characteristics, and performance by adjusting laser power, speed, and hatch distance to meet application requirements.

Design of Experiments

The design has four two-level factors: laser power (P) (370 and 390 w/s), speed (v) (1000 and 1500 m/sec), and hatch distance (h_d) (0.19 and 0.21 mm) across two materials. Compression strength (KN) and fatigue (MPa) are response variables. The fatigue and compression tests were conducted using an INSTRON Testing machine to evaluate the mechanical properties of DMLS processed AlSi and AlSi10Mg samples. For the fatigue test, specimens were subjected to cyclic loading at a frequency of 10 Hz with a stress ratio (R) of 0.1 until failure, following ASTM E466 standards. Compression tests were performed according to ASTM E9, with specimens compressed at a constant strain rate of 0.005 s until yielding or failure. The tests were carried out at room temperature, and data acquisition captured load, displacement, and cycles to failure. Surface roughness was measured pre and post testing to correlate mechanical performance with surface quality. The results highlighted that higher laser power improved both compression strength and fatigue resistance, with AlSi10Mg samples outperforming AlSi in most conditions. The Taguchi approach generates 16 tests from a complete factorial design of 25 to standardise experimentation factors [10]. ANOVA shows that scan speed, laser power, and hatch distance affect response variables, revealing their individual and combined impacts on observed variances. The experimental data is presented in Table 2.

Table 2 encapsulates a comprehensive dataset detailing various experimental runs conducted under differing conditions, including laser power, speed, hatch distance, and material type, each with associated predictions for compression strength and fatigue. The integration of grey relational analysis (GRA) into the assessment of this data yields a nuanced understanding of the relationships between these parameters and the predicted outcomes. By calculating grey relational grade (GRG) values for each run, the analysis effectively quantifies the degree of similarity between the predicted and experimental results, thereby facilitating the identification of optimal parameter combinations.

Grey relational analysis (GRA) is a method used to analyse the relationships between multiple factors and a response variable in a system or process. It is often used in conjunction with Taguchi's array to evaluate the influence of factors on a system's performance. In GRA, the grey relational coefficient (GRC) is calculated to quantify the similarity between the experimental data and a reference sequence. The higher the GRC value, the stronger the relationship between the factor level and the response variable [11].

The general formula for calculating the grey relational coefficient (GRC) in Taguchi's analysis is as follows:

$$\xi = \frac{min\left(y_{P1}, y_{e1}\right) + \alpha \cdot max\left(y_{P2}, y_{e2}\right)}{y_{P1} + \alpha y_{e1}}$$

where,

- ξ is the grey relational coefficient between predicted and experimental values

Table 2 Results obtained with optimized process parameters

Run	Laser power	Speed (mm/sec)	Hatch distance (mm)	Material	Surface roughness (µm)	Predicted		Experimental		GRG	GRG Rank
						Compression strength (y_{p1}) (KN)	Fatigue (y_{p2}) (MPa)	Compression strength (y_{e1}) (KN)	Fatigue (y_{e2}) (MPa)		
1	370	1000	0.19	Al-Si	0.65	0.377	192.2	51.02	39,856	3.726	11
2	370	1000	0.19	Al-Si-10 Mg	0.8	0.464	120.4	55	25,689	2.169	15
3	370	1000	0.21	Al-Si	0.7	0.439	221.4	54.01	45,685	4.049	7
4	370	1000	0.21	Al-Si-10 Mg	1.2	0.622	108.5	59.36	23,100	1.81	16
5	370	1500	0.19	Al-Si	0.75	0.668	190.7	60.23	39,552	3.119	14
6	370	1500	0.19	Al-Si-10 Mg	0.54	0.364	198.1	50.25	41,025	3.9	9
7	370	1500	0.21	Al-Si	1.68	0.333	172.2	48.25	35,848	3.533	12
8	370	1500	0.21	Al-Si-10 Mg	1.44	0.392	198	51.84	41,000	3.777	10
9	390	1000	0.19	Al-Si	1.8	0.46	237.8	54.82	48,965	4.282	5
10	390	1000	0.19	Al-Si-10 Mg	1.65	0.423	280	53.32	56,000	5.184	2
11	390	1000	0.21	Al-Si	0.47	0.345	222.1	49.09	45,825	4.475	4
12	390	1000	0.21	Al-Si-10 Mg	0.65	1	267.1	64.2	54,826	4.064	6
13	390	1500	0.19	Al-Si	0.98	0.468	195	55.15	39,000	3.493	13
14	390	1500	0.19	Al-Si-10 Mg	0.48	0.43	215.8	53.65	44,568	3.974	8
15	390	1500	0.21	Al-Si	0.25	0.359	248	49.98	51,002	4.905	3
16	390	1500	0.21	Al-Si-10 Mg	0.23	0.48	320.4	55.56	65,482	5.685	1

- y_{p1} and y_{p2} are the predicted values
- y_{e1} and y_{e2} are the experimental values
- $\min(y_p, y_e)$ is the minimum value between the predicted and experimental values
- $\max(y_p, y_e)$ is the maximum value between the predicted and experimental values
- α is the distinguishing coefficient

Within this framework, the grey relational grade (GRG) rank assigned to each run serves as a crucial metric, signifying its relative performance compared to others in the dataset. A lower GRG value corresponds to a higher rank, indicating a stronger alignment between predicted and experimental outcomes. For instance, run 16 emerges as the top performer, boasting a GRG rank of 1, which suggests exceptional congruence between its predicted and actual results. Conversely, run 2 exhibits the least favourable performance, characterized by a comparatively higher GRG rank, denoting a larger discrepancy between its predicted and observed outcomes. The higher compression strength and fatigue values would imply that the manufactured parts or components are stronger and more durable than what was predicted based on theoretical or simulation models. While predictive models and simulations are valuable tools for initial design and optimization, real-world testing is essential to validate these predictions and ensure that the manufactured parts meet the required specifications and performance criteria.

This refined analysis not only elucidates the effectiveness of individual parameter configurations in achieving the desired material properties, but also provides valuable insights into the broader optimization of manufacturing processes. By discerning the impact of each parameter on the predicted outcomes and their subsequent experimental validation, stakeholders can make informed decisions regarding process refinement and parameter optimization, thereby enhancing overall efficiency and product quality in industrial settings.

The "GRG Rank" column ranks samples by performance across these factors. Lower rankings indicate better achievement. While certain parameters' anticipated values are close to actual measurements, discrepancies remain, indicating areas where prediction models need additional study or modification.

Results and Discussions

Surface roughness

Surface roughness measurements offered understanding into how process variables impacted the external surface quality of components [12]. The analysis of variance emphasized the preference for smaller values, as indicated by the significance of all factors with *p* values below 0.10. The Delta ranking, outlined in Table 3, distinctly illustrates the influence of laser power followed by scanning speed on surface roughness Ra. This underscores the preference for smaller values, as evidenced by the surface roughness values obtained for S/N ratios [13], as depicted in Fig. 2a and b.

Compression strength

Compression strength exhibited a strong dependence on hatch distance. Lower hatch distances resulted in increased compression strength due to higher density and reduced

Table 3 Analysis of variance for S/N ratios, $R^2 = 98.1\%$

Source	DF	Sum of squares	F	p	Statistical significance
Laser power	1	38.533	23.23	0.005	High
Scan speed	1	34.503	20.80	0.006	Low
Hatching distance	1	20.979	12.65	0.016	Low
Material	1	0.413	0.25	0.639	High
Residual error	5	8.295			
Total	15				

| (a) surface roughness plots for laser power & scan speed | (b) surface roughness plots for hatching distance& material |
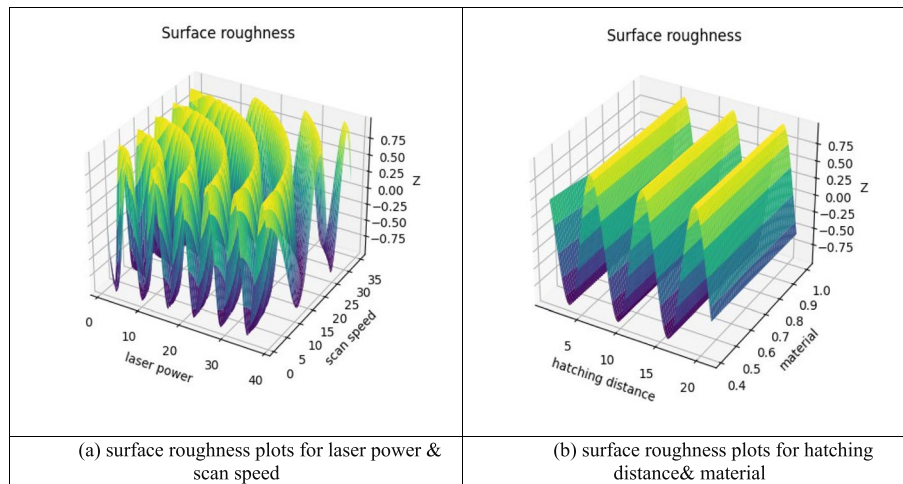
Fig. 2 **a** Surface roughness plots for laser power and scan speed. **b** Surface roughness plots for hatching distance and material

porosity. Laser power and scan speed also influenced compression strength to a lesser extent [14]. Larger is better.

Similarly, as can be shown in the Fig. 3a and b, all components are significant in the analysis off variance for S/N ratios since their *p* values are less than 0.10. In this case of analysing the variance, the Delta ranking obtained from the Table 4 clearly shows that the laser power has significant effect on the compression strength with rank 1, hatching distance showing the second significant affect with ranking order 2, material being rank order 3, and scanning speed showing very less effect on the compression strength.

Fatigue resistance

Fatigue tests demonstrated a complex relationship between process parameters and fatigue resistance. At certain parameter combinations, improved fatigue behaviour was observed due to optimized microstructure. However, some combinations led to surface irregularities that accelerated crack propagation [14]. Larger is better.

In a similar vein, Fig. 4a and b demonstrate that, according to the analysis off variance for S/N ratios, all components are significant because their p values are smaller than 0.10. In this case of analysing the variance, the Delta ranking obtained from the Fig. 4 clearly shows that the Laser power has significant effect on the compression
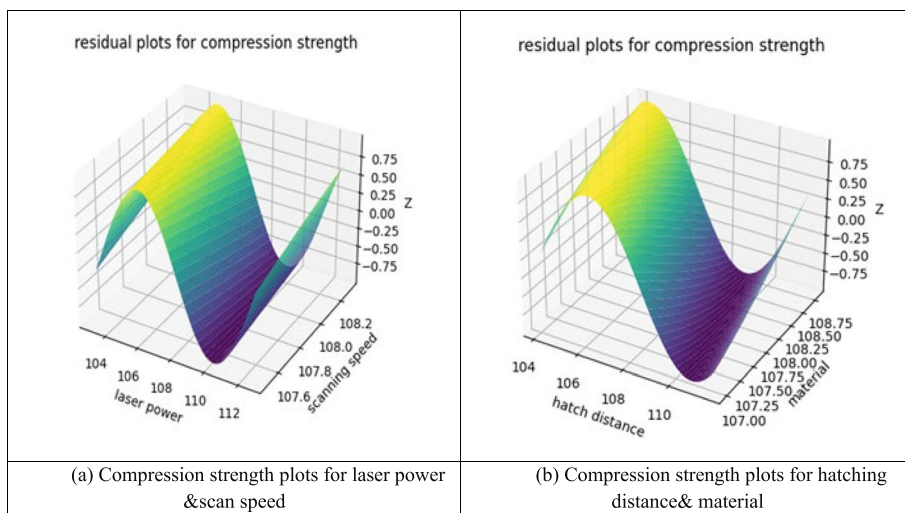
(a) Compression strength plots for laser power &scan speed

(b) Compression strength plots for hatching distance& material

Fig. 3 **a** Compression strength plots for laser power and scan speed. **b** Compression strength plots for hatching distance and material

Table 4 S/N mean response for compression strength

S. No	Laser power	Scanning speed	Hatch distance	Material
1	103.1	108.3	104.1	107.0
2	112.6	107.5	111.6	108.8
Delta	9.5	0.8	7.5	1.8
Rank	1	4	2	3

(a) Fatigue plots for laser power &scan speed

(b) Fatigue plots for hatching distance& material
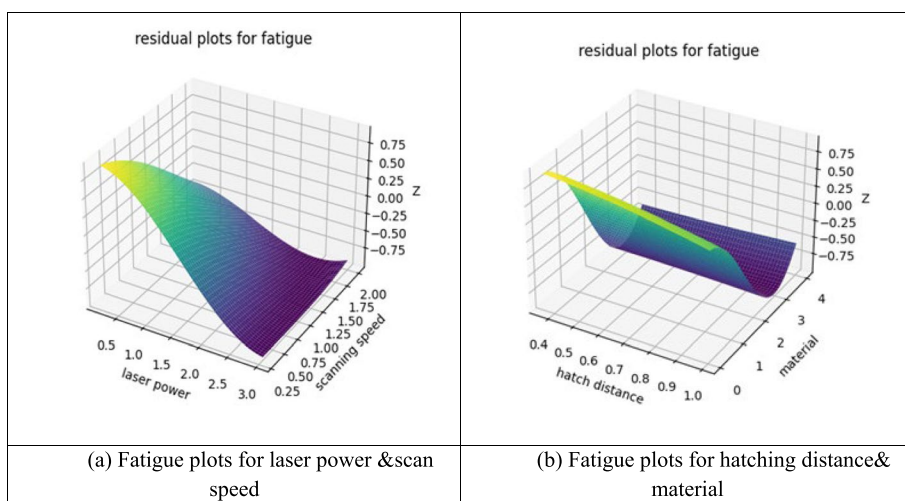
Fig. 4 **a** Fatigue plots for laser power and scan speed. **b** Fatigue plots for hatching distance and material

strength with rank 1, hatching distance showing the second significant affect with ranking order 2, material being rank order 3, and scanning speed showing very less effect on the compression strength from the response mean (Table 5).

Table 5 S/N mean response for fatigue resistance

S. No	Laser power	Scanning speed	Hatch distance	Material
1	34.72	34.80	34.82	34.66
2	34.56	34.48	34.46	34.62
Delta	0.17	0.32	0.37	0.04
Rank	3	2	1	4

Process variable optimization

Combining ANOVA and GRA data helped find optimal process parameters. Fatigue and compression studies assessed DMLS-produced metal components' mechanical characteristics [15, 16]. Table 2 indicated a strong link between process parameters and mechanical reactions [17, 18]. Table 2 compares 16 samples projected and experimental compression strength (KN) and fatigue (MPa). Most anticipated values match experimental data; however, there are some discrepancies.

- Surface roughness (μm): Predicted values range from 0.333 to 1.000, whereas experimental values range from 0.23 to 1.68 μm. Predicted values are generally close to experimental, except for a few instances with larger disparities.
- Compression strength (kN): Predicted values range from 0.333 to 1.000 kN, whereas experimental values are 48.25 to 64.2 KN. The anticipated and experimental values differ, especially at extremes. Hatch distance strongly affected compression strength. Higher density and decreased porosity enhanced compression strength at lower hatch spacing. Lighter effects of laser power and scan speed on compression strength.
- Fatigue (MPa): Predicted values 0.438–0.763 MPa; experimental values, 23,100–65,482 MPa. Most samples show large variations between expected and experimental values. Process factors affect fatigue resistance in complicated ways, according to fatigue testing. Optimisation of microstructure enhanced fatigue behaviour for specific parameter combinations.

Microstructural analysis

FESEM was used to examine how process factors affected AlSi10Mg ($100 \times 50 \times 10$ mm) component surface roughness after DMLS fabrication. The higher laser power at lower scan rates and moderate hatch spacing reduces layer voids [19]. Figure 5a, b and c and d show how laser power improves surface finish, fatigue resistance, and compression strength. At 390 W/s, the grain structure is finer than at 370 W/s, indicating fewer microvoids.

Figure 5c and d show the surface morphological variation. The shorter hatching distance, slower scanning speed, and greater laser power may eliminate cavities or necks between scanning tracks, enhancing the surface [20]. The hatching process was studied using FESEM. Thus, better process parameters may strengthen items with poorer surface finishes. FESEM was used to study how various factors affected DMLS-made
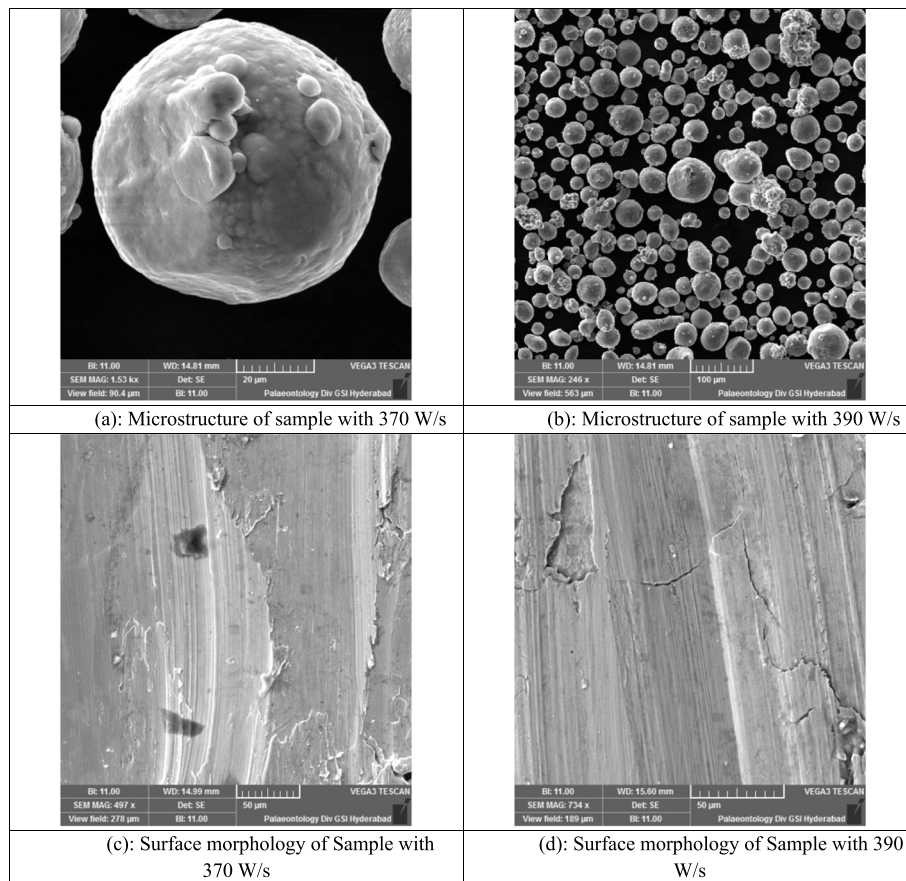
(a): Microstructure of sample with 370 W/s	(b): Microstructure of sample with 390 W/s
(c): Surface morphology of Sample with 370 W/s	(d): Surface morphology of Sample with 390 W/s

Fig. 5 **a** Microstructure of sample with 370 W/s. **b** Microstructure of sample with 390 W/s. **c** Surface morphology of sample with 370 W/s. **d** Surface morphology of sample with 390 W/s

AlSi10Mg components' hardness, surface roughness, fatigue, compression strength, and tensile strength. DMLS-produced components' intrinsic structure was revealed via microstructural investigation. Grain size, porosity, and phase distribution varied with parameter combinations. Smaller grain sizes were reported with greater laser powers and lower scan rates. This was due to increased energy input and regulated solidification. High scan speeds increased porosity due to inadequate energy input for fusion. Reduced porosity and increased density were achieved via optimal hatch distance.

Conclusions

This study emphasises the relevance of process parameters in affecting DMLS metal component mechanical qualities, microstructure, and surface features.

- Higher laser power (390 W) generally resulted in higher compression strength and better fatigue resistance, as seen in the top-ranked runs (e.g. runs 16 and 10).
- Al-Si-10 Mg samples frequently outperformed Al-Si samples in terms of mechanical properties like compression strength and fatigue resistance, indicating that adding magnesium enhances the material's overall performance (e.g. runs 16, 10, and 4).

- Optimal combinations of process parameters, such as a laser power of 390 W, a speed of 1500 mm/sec, and a hatch distance of 0.21 mm, led to the best mechanical performance, with run 16 achieving the highest grey relation grade (GRG) of 5.685.
- Lower surface roughness values were generally associated with better mechanical performance, suggesting that optimizing laser power and speed improves both strength and fatigue resistance as well as surface quality (e.g. runs 10 and 11).

Reproducing the printing process with the desired parameters confirmed the ideal parameter combinations. The components were tested against optimisation predictions. The study examined how scan speed, laser power, and hatch distance affect DMLS-produced metal component qualities using this thorough experimental methodology. The results showed that, in summary, increasing laser power in DMLS may potentially improve compression strength, and fatigue resistance by promoting better fusion between powder particles and optimizing the microstructure. However, it is crucial to carefully control the laser parameters to avoid introducing defects or other detrimental effects that may compromise the mechanical properties of the printed parts. Statistical research using grey relation analysis examined how process parameters affect AlSi0Mg samples' mechanical properties. Laser power was the biggest factor impacting mechanical properties, microstructure, and surface roughness. The "smaller-the-better" S/N ratio was used for surface roughness evaluation, whereas the "larger is better" equation was used for compression strength and fatigue.

Abbreviations

ANOVA	Analysis of variance
DMLS	Direct metal laser sintering
FESEM	Finite element scanning electron microscope
GRA	Grey relational analysis
GRC	Grey relational coefficient
GRG	Grey relational grade
kN	Kilonewton
MPa	Megapascal
S/N ratio	Signal-to-noise ratio

Declarations

Competing interests
The authors declare that they have no competing interests.

References

1. Alsalla HH, Smith C, Hao L (2018) The effect of different build orientations on the consolidation, tensile and fracture toughness properties of direct metal laser sintering Ti-6Al-4V. Rapid Prototyping Journal 24(2):276–284
2. Kushwaha AK, Rahman MH, Slater E, Patel R, Evangelista C, Austin E, Tompkins E, McCarroll A, Rajak DK, Menezes PL (2022) Powder bed fusion–based additive manufacturing: SLS, SLM, SHS, and DMLS. In Tribology of Additively Manufactured Materials (pp. 1–37). Elsevier
3. Fuchs D, Bartz R, Kuschmitz S, Vietor T (2022) Necessary advances in computer-aided design to leverage on additive manufacturing design freedom. International Journal on Interactive Design and Manufacturing (IJIDeM) 16(4):1633–1651
4. Hirsch M, Patel R, Li W, Guan G, Leach RK, Sharples SD, Clare AT (2017) Assessing the capability of in-situ nondestructive analysis during layer based additive manufacture. Addit Manuf 13:135–142
5. Kunisetti P, Prasad BS, Mouli KVC (2023) Influence of varied laser density on sintering processing parameters, mechanical properties, and microstructural characteristics of DMLS-printed AlSi10Mg materials: a comparative experimental study. Transactions of the Indian Institute of Metals, pp.1–9
6. Li J, Wang Q, Michaleris P (2018) An analytical computation of temperature field evolved in directed energy deposition. J Manuf Sci Eng 140(10):101004
7. Qin Y, Qi Q, Shi P, Scott PJ, Jiang X (2023) Selection of materials in metal additive manufacturing via three-way decision-making. The International Journal of Advanced Manufacturing Technology 126(3–4):1293–1302
8. Alsalla HH, Smith C, Hao L (2018) Effect of build orientation on the surface quality, microstructure and mechanical properties of selective laser melting 316L stainless steel. Rapid prototyping journal 24(1):9–17
9. Laureijs RE, Roca JB, Narra SP, Montgomery C, Beuth JL, Fuchs ER (2017) Metal additive manufacturing: cost competitive beyond low volumes. J Manuf Sci Eng 139(8):081010
10. Yang B, Lai Y, Yue X, Wang D, Zhao Y (2020) Parametric optimization of laser additive manufacturing of Inconel 625 using Taguchi method and grey relational analysis. Scanning 2020:e9176509
11. Agapovichev AV, Khaimovich AI, Smelov VG, Kokareva VV, Zemlyakov EV, Babkin KD, Kovchik AY (2023) Multiresponse optimization of selective laser melting parameters for the Ni-Cr-Al-Ti-based superalloy using gray relational analysis. Materials 16(5):2088
12. Calignano F, Manfredi D, Ambrosio EP, Iuliano L, Fino P (2013) Influence of process parameters on surface roughness of aluminum parts produced by DMLS. Int J Adv Manufac Technol 67(9):2743–2751
13. Márquez C, López JD, Cabrera L, González L, Botana J (2021) Study of the influence of laser energy density on the surface roughness of Scalmalloy ® Samples Manufactured by DMLS Technology. IOP Conference Series: Materials Science and Engineering 1193(1):012036
14. Seshagirirao DV, Raju S, Mantrala KM (2023) Evaluation of compression, wear and electrochemical behavior of CoCrMo alloy samples fabricated with direct metal laser sintering. J Mater Eng Perform 32(17):7633–7639
15. Leon A, Aghion E (2017) Effect of surface roughness on corrosion fatigue performance of AlSi10Mg alloy produced by selective laser melting (SLM). Mater Charact 131:188–194
16. Nicoletto G, Konečná R, Kunz L, Frkáň M (2018) "Influence of As-built surface on fatigue strength and notch sensitivity of Ti6Al4V alloy produced by DMLS" edited by G. Hénaff MATEC Web of Conferences 165:02002
17. Winowlin Jappes JT (2022) Solid particle erosion studies on heat treated SU718 alloy developed through DMLS processed additive manufacturing. Advances in Materials and Processsing Technologies 8(3):2672–2683
18. Raj BA, Jappes JW, Khan MA, Dillibabu V, Brintha NC (2020) Direct metal laser sintered (DMLS) process to develop Inconel 718 alloy for turbine engine components. Optik 202:163735
19. Raj BA, Jappes JW, Khan MA, Dillibabu V, Brintha NC (2019) Studies on heat treatment and electrochemical behaviour of 3D printed DMLS processed nickel-based superalloy. Appl Phys A 125:1–8
20. Ruban R, Rajashekhar VS, Nivedha B, Mohit H, Sanjay MR, Siengchin S (2022) Role of additive manufacturing in biomedical engineering. Innovations in additive manufacturing. Springer International Publishing, Cham, pp 139–157

Publisher's Note